

Hindawi Publishing Corporation  
The Scientific World Journal  
Volume 2014, Article ID 408613, 8 pages  
<http://dx.doi.org/10.1155/2014/408613>



## Research Article

# In-Band Asymmetry Compensation for Accurate Time/Phase Transport over Optical Transport Network

**Sammy Siu, Wen-Hung Tseng, Hsiu-fang Hu, Shinn-Yan Lin,  
Chia-Shu Liao, and Yi-Liang Lai**

*Telecommunication Laboratories, Chunghwa Telecom Co., Ltd., No. 99, Dianyan Road, Taoyuan County,  
Yangmei City 32601, Taiwan*

Correspondence should be addressed to Wen-Hung Tseng; [whtseng@cht.com.tw](mailto:whtseng@cht.com.tw)

Received 2 January 2014; Accepted 19 March 2014; Published 10 April 2014

Academic Editors: H. R. Karimi, X. Yang, and Z. Yu

Copyright © 2014 Sammy Siu et al. This is an open access article distributed under the Creative Commons Attribution License, which permits unrestricted use, distribution, and reproduction in any medium, provided the original work is properly cited.

The demands of precise time/phase synchronization have been increasing recently due to the next generation of telecommunication synchronization. This paper studies the issues that are relevant to distributing accurate time/phase over optical transport network (OTN). Each node and link can introduce asymmetry, which affects the adequate time/phase accuracy over the networks. In order to achieve better accuracy, protocol level full timing support is used (e.g., Telecom-Boundary clock). Due to chromatic dispersion, the use of different wavelengths consequently causes fiber link delay asymmetry. The analytical result indicates that it introduces significant time error (i.e., phase offset) within 0.3397 ns/km in C-band or 0.3943 ns/km in L-band depending on the wavelength spacing. With the proposed scheme in this paper, the fiber link delay asymmetry can be compensated relying on the estimated mean fiber link delay by the Telecom-Boundary clock, while the OTN control plane is responsible for processing the fiber link delay asymmetry to determine the asymmetry compensation in the timing chain.

## 1. Introduction

Precise synchronization of clocks has become an important technique not only for the scientific researches but also for the modern daily life. For many industrial infrastructures, the demands for precise time/phase synchronization have greatly increased recently, for example, communication networks, the smart grid of electric power distribution systems [1], and the practice of providing time stamps for financial networks [2]. Traditional communication network synchronization has relied on the accurate distribution of frequency [3]; evolving wireless networks require the distribution of accurate time/phase based on IEEE1588v2 for long term evolution (LTE) and accurate quality-of-service/service-level-agreement (QoS/SLA) measurements to determine the network health [4, 5].

The primary reference time clocks (PRTC) location depends on the network that IEEE1588v2 support. Currently, the PRTCs are closer to the end application than the primary reference clocks (PRCs) for traditional frequency

distribution, in order to limit and control time/phase degradation [6]. The core networks will incorporate the accurate time/phase distribution capability into optical transport network (OTN), as addressed in ITU-T Recommendation G.709 [7]. The OTN provides new packet based time/phase distribution service; thus the PRTCs can collocate with the PRCs as shown in Figure 1. This architecture is compatible with PRTC redundancy (e.g., in order to secure the global navigation satellite system (GNSS) failures) and also requires a small number of GNSS receivers. The integrity of transferring accurate time/phase synchronization distribution over OTN in the core network and packet transport network with synchronous ethernet (PTN with Sync-E) in the backhaul networks [8, 9] can simplify network architecture, reduce operational expenditure (OPEX), and make the network easy to maintain.

For accurate time/phase transport over OTN, two options are considered: (1) the use of OTN optical channel data unit-k (ODUK) reserved overhead bytes to transport IEEE1588v2 Sync packets as shown in Figure 2 and (2) the use of optical supervisory channel (OSC) to transport IEEE1588v2 Sync

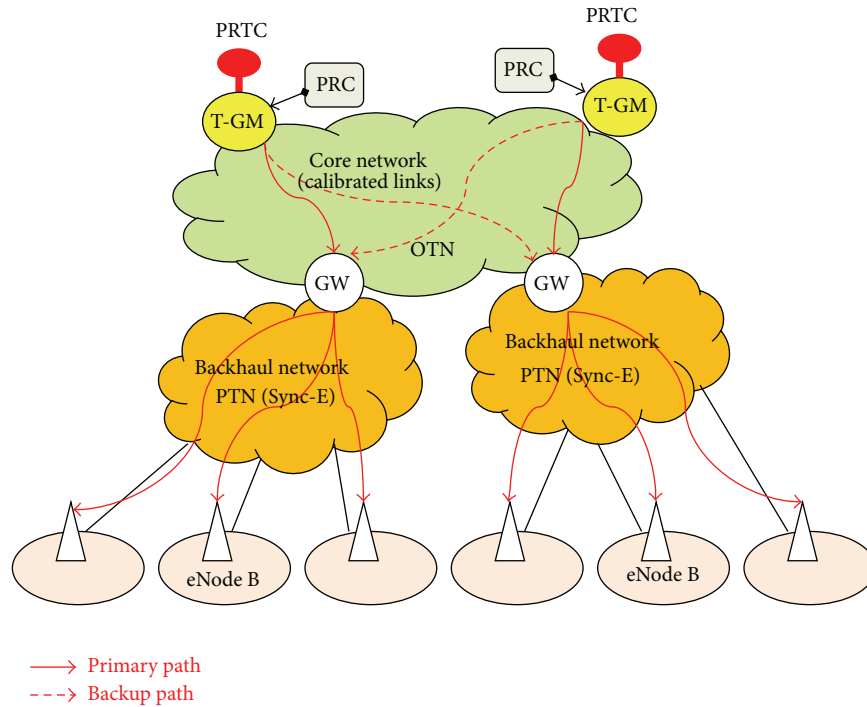


FIGURE 1: Architecture with centralized PRTC functions collocated with PRC. T-GM: telecom-grand master; GW: gate way.

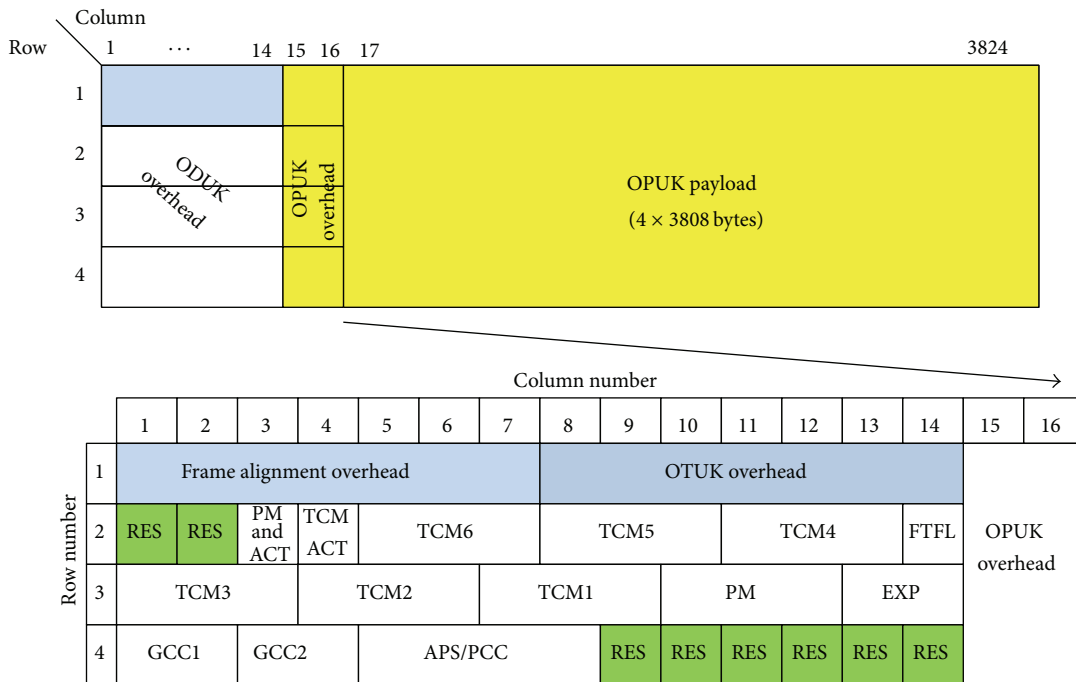


FIGURE 2: Optical transport network (OTN) frame format (ITU-T G.709).

packets [10]. The former belongs to In-band and the latter belongs to Out-of-band [7].

Nevertheless, each node and link can introduce asymmetry, which affects the adequate time/phase accuracy over the networks. Removal of packet delay variation (PDV) and asymmetry in the OTN nodes by means of IEEE1588v2

support (e.g., T-BC in every node [11, 12]) is analogue to backhaul network (ITU-T G.8275.1). In OTN, the forward and backward paths may not be the same wavelength depending on network configuration or wavelength switching; this will result in fiber link delay asymmetry and should be taken into account.

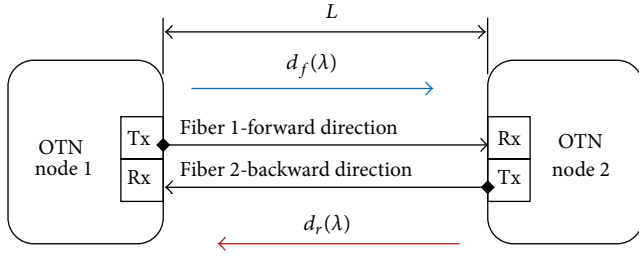


FIGURE 3: Packet signal transmission over optical fiber links.

In this paper, we focus on the use of OTN overhead to transport Sync packets (In-band). The link delay asymmetry formation is given in Section 2, removal link and node asymmetry based on T-BC mode is given in Section 3, and the link delay asymmetry analysis is given in Section 4.

## 2. Use of Different Wavelengths

In wavelength division multiplexing (WDM), multiple channels of information carried over the same fiber each using an individual wavelength to increase the transmission capacity as shown in Figure 3. Due to chromatic dispersion, the use of different wavelengths consequently causes fiber link delay asymmetry [13]. Group velocity is given by  $v = c/\eta$ , where  $c$  is speed of light and  $\eta$  is group refractive index depending on wavelength ( $\lambda$ ). The fiber link delay asymmetry is given by

$$A(\lambda) = d_f(\lambda) - d_r(\lambda) = L \times \left( \frac{\eta_f(\lambda)}{c} - \frac{\eta_r(\lambda)}{c} \right), \quad (1)$$

where  $L$  denotes the transmission distance (fiber link length),  $d_f, d_r$  are forward and backward propagation delays, and  $\eta_f, \eta_r$  are the related refractive indexes. The mean fiber link delay ( $D$ ) can be represented as

$$D = \frac{L}{2} \times \left( \frac{\eta_f(\lambda)}{c} + \frac{\eta_r(\lambda)}{c} \right). \quad (2)$$

Then,

$$L = \frac{2D}{\eta_f(\lambda)/c + \eta_r(\lambda)/c}. \quad (3)$$

Substituting  $L$  in (3) into (1) and simplifying, one obtains the fiber link delay asymmetry in terms of network mean fiber link delay as follows:

$$A(\lambda) = d_f(\lambda) - d_r(\lambda) = 2D \times \left( \frac{\eta_f(\lambda) - \eta_r(\lambda)}{\eta_f(\lambda) + \eta_r(\lambda)} \right). \quad (4)$$

Half of the delay asymmetry (i.e.,  $A(\lambda)/2$ ) will contribute to the time error, where  $A(\lambda)$  depends on the wavelength spacing.

## 3. Scheme to Remove Asymmetry Error of Node and Link

In IEEE1588v2 distribution, assume that the fiber link delay in each direction is symmetric, whereas in WDM systems

the delay may not be symmetric. Fortunately, if a T-BC is implemented in every node in OTN, the mean fiber link delay  $D$  can be estimated by the T-BC mode, which would know the difference  $(d_f(\lambda) - d_r(\lambda))$  to compensate the phase offset ( $\theta$ ) as shown in (4). The compensation scheme is proposed as follows.

**3.1. Telecom-Boundary Clock Mode.** Each node and link in a network can introduce asymmetry. In Telecom-Boundary clock (T-BC) mode [14], ingress/egress buffers are bypassed, and nodes asymmetry is avoided as shown in Figure 4. The time transfer model as shown in Figure 5 can be written as

$$\begin{aligned} T_2 &= T_1 + \theta + \delta_{\text{link},M \rightarrow S}, \\ T_4 &= T_3 - \theta + \delta_{\text{link},S \rightarrow M}, \end{aligned} \quad (5)$$

where  $\delta_{\text{node}}, \delta_{\text{link}}$  denote node and link delay, respectively, and assume  $\delta_{\text{node},M \rightarrow S} = \delta_{\text{node},S \rightarrow M}$ .

Based on the time transfer model in (5), the estimated mean fiber link delay  $\widehat{D}$  and estimated phase offset  $\widehat{\theta}$  can be derived as

$$\widehat{D} = \frac{\delta_{\text{link},M \rightarrow S} + \delta_{\text{link},S \rightarrow M}}{2} = \frac{(T_2 - T_1) + (T_4 - T_3)}{2}, \quad (6)$$

$$\widehat{\theta} = \frac{(T_2 - T_1) - (T_4 - T_3)}{2} - \frac{(\delta_{\text{link},M \rightarrow S} - \delta_{\text{link},S \rightarrow M})}{2}. \quad (7)$$

Equation (7) shows that any asymmetry will contribute with half of that to the error in the phase offset calculation. The second term in (7) is the link asymmetry compensation. The link asymmetry consists of mainly fiber link length asymmetry and fiber link delay asymmetry for use of different wavelengths. Substituting  $\widehat{D}$  in (6) into (4), assume that the fiber link length is symmetric; one obtains the fiber link delay asymmetry as

$$A(\lambda) = ((T_2 - T_1) + (T_4 - T_3)) \times \left( \frac{\eta_f(\lambda) - \eta_r(\lambda)}{\eta_f(\lambda) + \eta_r(\lambda)} \right). \quad (8)$$

Substituting (8) into (7), one obtains the estimated phase offset  $\widehat{\theta}$  as

$$\begin{aligned} \widehat{\theta} &= \left( \frac{(T_2 - T_1) - (T_4 - T_3)}{2} \right) - \frac{1}{2} ((T_2 - T_1) + (T_4 - T_3)) \\ &\quad \times \left( \frac{\eta_f(\lambda) - \eta_r(\lambda)}{\eta_f(\lambda) + \eta_r(\lambda)} \right). \end{aligned} \quad (9)$$

The second term in (9) represents the fiber link delay asymmetry compensation. If the same wavelength is used both on forward and backward paths (i.e.,  $\eta_f(\lambda) = \eta_r(\lambda)$ ), then (9) becomes

$$\widehat{\theta} = \left( \frac{(T_2 - T_1) - (T_4 - T_3)}{2} \right). \quad (10)$$

If there is a fiber length difference  $\beta$  between forward and backward paths, this will cause  $\beta \cdot \eta(\lambda)/2c$  error in

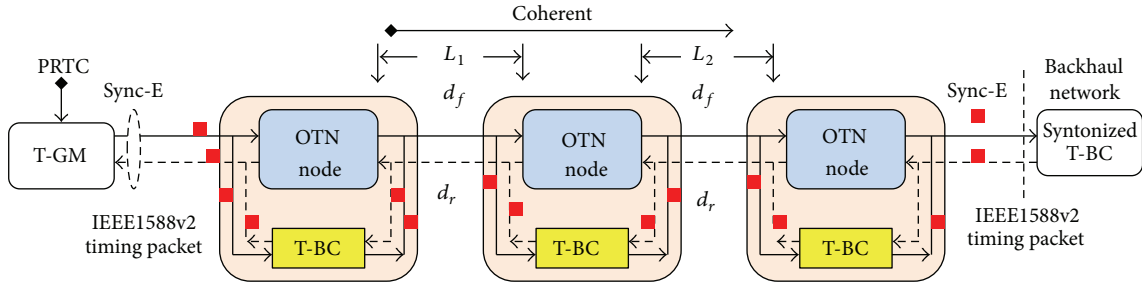


FIGURE 4: Telecom-Boundary clock mode in OTN.

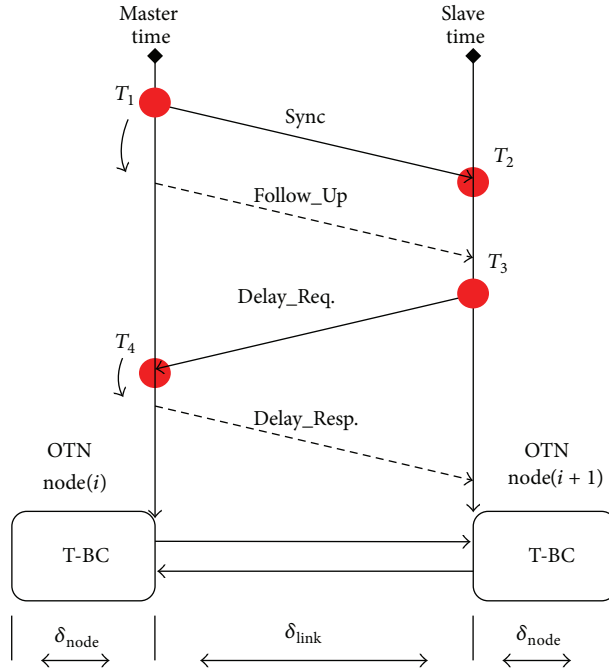


FIGURE 5: Time transfer mode based on T-BC mode

the estimation of phase offset  $\hat{\theta}$ . For example, when  $\eta$  is 1.4682 at  $\lambda = 1550$  nm, the estimated phase offset will have about 2.449 ns of error per meter of length asymmetry, which is related to the group delay (about 4.897 ns per meter).

**3.2. Reducing Link Length Asymmetry.** In a practical communication network, the link length asymmetry could be diminished to a tolerable extent if the fiber links are well designed at the beginning. An illustration of bidirectional and unidirectional protection switches in existent network fault management is shown in Figure 6. Bidirectional protection switch can minimize link length asymmetry ( $\beta$ ) because two-way time transfer (TWTT) takes place within one cable. The cable asymmetry  $\beta$  should be within two meters ( $\beta < 2$  m); this requires good cabling control. However, unidirectional protection switch TWTT takes place in separate cables, where the working and protection cables may not be in equal link length (i.e.,  $L_w \neq L_p$ ). In the current field trials, some budget is allocated for link length asymmetry unless the accurate link length asymmetry is manually measured and compensated.

#### 4. In-Band Link Delay Asymmetry Analysis

The dispersion of single-mode optical fiber (e.g., SMF-28 that meets the requirements of ITU-T Recommendation G. 652) is

$$\bar{D}(\lambda) = \frac{\lambda S_o}{8} \left( 1 - \frac{\lambda_o^4}{\lambda^4} \right), \quad (11)$$

where  $S_o$  ( $\leq 0.092$  ps/(nm<sup>2</sup>·km)) is the zero dispersion slope,  $\lambda_o$  ( $1302$  nm  $\leq \lambda_o \leq 1322$  nm) is the zero dispersion wavelength ( $\lambda_o = 1310$  nm in the following calculation), and  $\lambda$  ( $1200$  nm  $\leq \lambda \leq 1600$  nm) is the operating wavelength [15]. The index of refraction  $\eta$  and  $\bar{D}(\lambda)$  are related by  $(1/c)(\partial\eta/\partial\lambda) = \bar{D}(\lambda)$ , which is then written as

$$\frac{\eta(\lambda)}{c} = \frac{\eta(\lambda_o)}{c} + \int_{\lambda_o}^{\lambda} \bar{D}(\lambda) d\lambda. \quad (12)$$

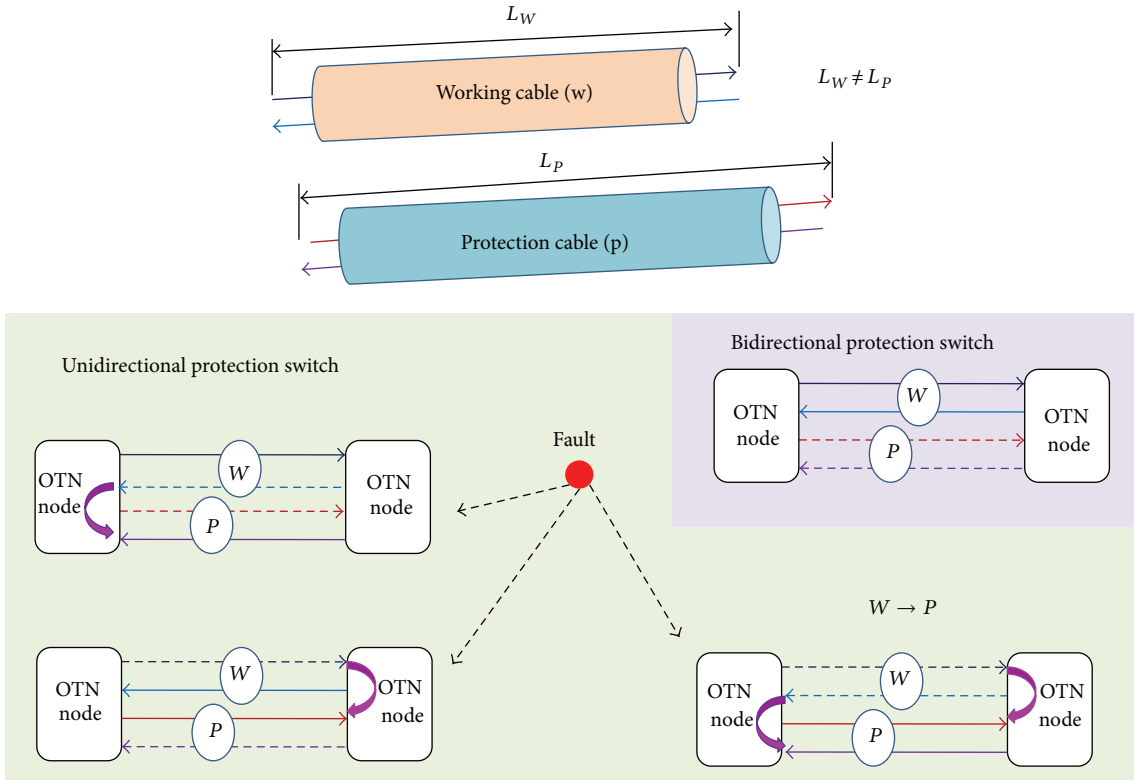


FIGURE 6: Schematic illustration of bidirectional/unidirectional network protection switches.

After integrating, we find that

$$\frac{\eta(\lambda)}{c} - \frac{\eta(\lambda_o)}{c} = \frac{S_o}{8} \lambda^2 \left( 1 - \frac{\lambda_o^2}{\lambda^2} \right)^2 \quad (13)$$

Substituting (13) into (1), the fiber link delay asymmetry per km ( $A/L$ ) is

$$\begin{aligned} \frac{A}{L} &= \frac{\eta_f(\lambda_f)}{c} - \frac{\eta_r(\lambda_r)}{c} \\ &= \frac{S_o}{8} \left\{ \lambda_f^2 \left( 1 - \frac{\lambda_o^2}{\lambda_f^2} \right)^2 - \lambda_r^2 \left( 1 - \frac{\lambda_o^2}{\lambda_r^2} \right)^2 \right\}, \end{aligned} \quad (14)$$

where  $\lambda_f$  and  $\lambda_r$  are the wavelengths in the forward and backward directions and are defined based on ITU wavelength grid specification. The fiber link delay asymmetry  $A(\lambda)$  depends on the wavelength spacing  $\{\lambda_f, \lambda_r\}$  and also fiber link length ( $L$ ) as shown in (14). The calculated values of  $A(\lambda)$  versus  $L(\text{km})$  for  $\{\lambda_f = 1569 \text{ nm}, \lambda_r = 1530 \text{ nm}\}$  in C-band and  $\{\lambda_f = 1610 \text{ nm}, \lambda_r = 1570 \text{ nm}\}$  in L-band are depicted in Figure 7.

Based on (14), the maximum fiber link delay asymmetry for the two extreme wavelengths is about  $A/L = 0.6795 \text{ ns/km}$  in C-band (i.e.,  $1530 \text{ nm} \leq \lambda \leq 1569 \text{ nm}$ ) and  $A/L = 0.78854 \text{ ns/km}$  in L-band (i.e.,  $1570 \text{ nm} \leq \lambda \leq 1610 \text{ nm}$ ). This link delay asymmetry introduces significant

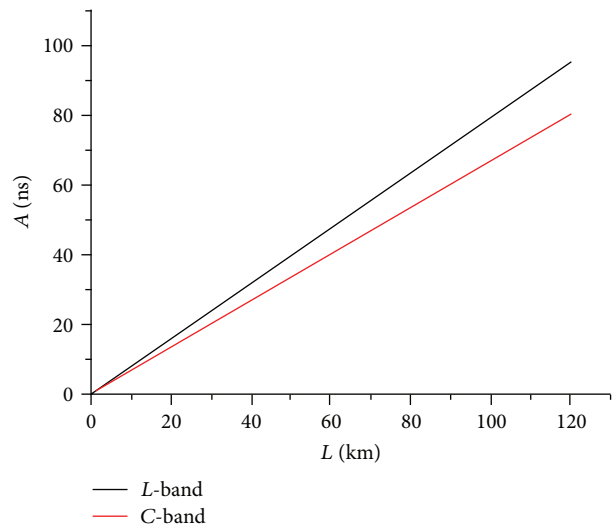


FIGURE 7: Fiber link delay asymmetry  $A(\lambda)$  versus transmission distance  $L(\text{km})$ , where  $\{\lambda_f = 1569 \text{ nm}, \lambda_r = 1530 \text{ nm}\}$  in C-band and  $\{\lambda_f = 1610 \text{ nm}, \lambda_r = 1570 \text{ nm}\}$  in L-band.

time error (i.e., phase offset) within  $0.3397 \text{ ns/km}$  in C-band (e.g.,  $L = 100 \text{ km}$ , phase offset  $\leq 33.97 \text{ ns}$ ) or  $0.3943 \text{ ns/km}$  in L-band (e.g.,  $L = 100 \text{ km}$ , phase offset  $\leq 39.43 \text{ ns}$ ). The above results are summarized in Table 1.

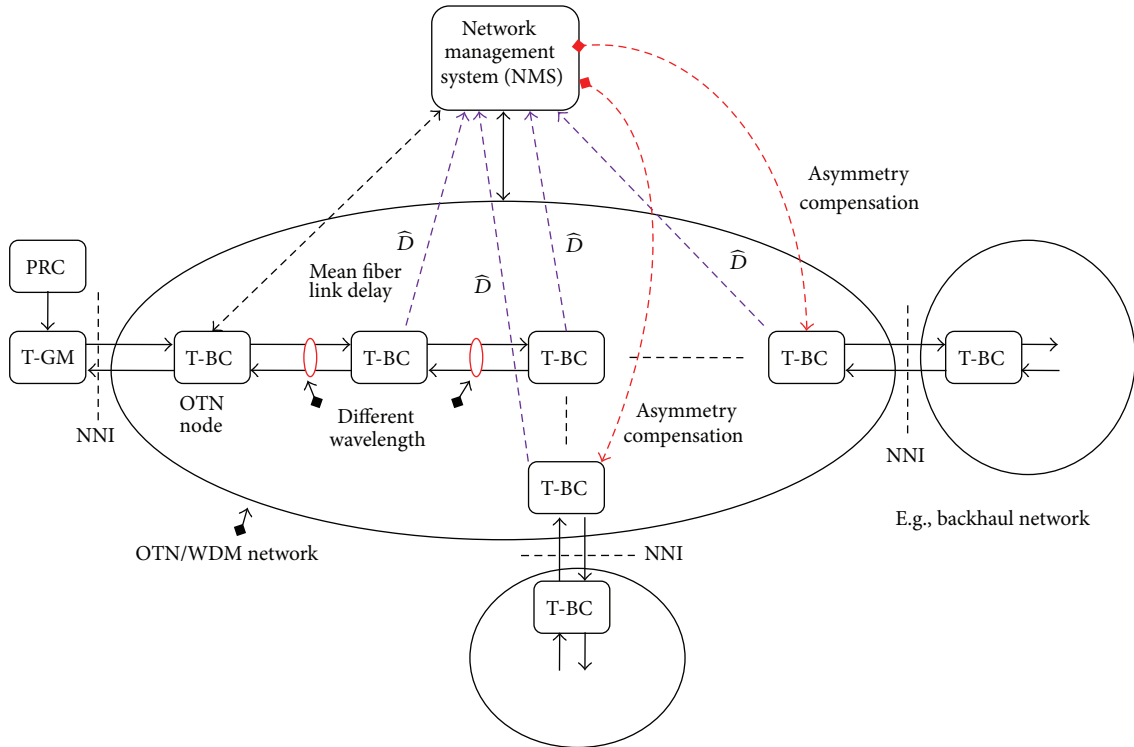


FIGURE 8: Asymmetry compensation support from control plane.

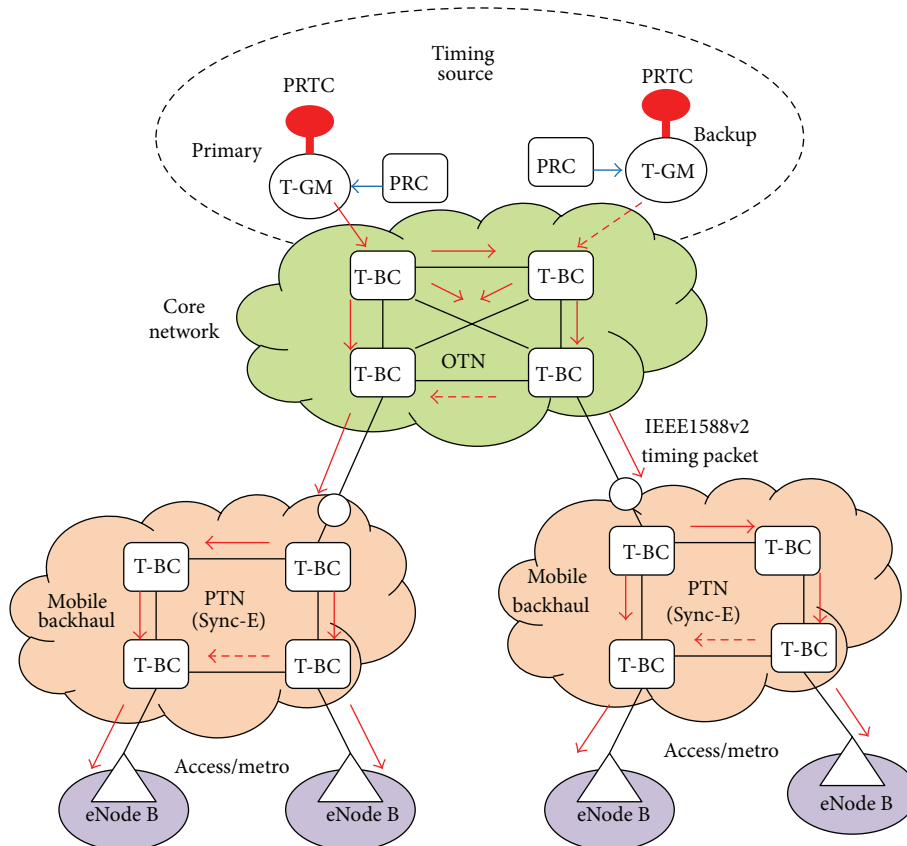


FIGURE 9: Time/phase over OTN networks with T-BC mode.



TABLE 1: Maximum fiber link delay asymmetry for the two extreme wavelengths.

Link delay asymmetry	C-band 1530 nm $\leq$ $\lambda$ $\leq$ 1569 nm	L-band 1570 nm $\leq$ $\lambda$ $\leq$ 1610 nm
$\frac{A(\lambda)}{L}$	$\leq 0.6795$ ns/km	$\leq 0.78854$ ns/km

For accurate time/phase transport, we have to take care of the fiber link delay asymmetry  $A(\lambda)$ , especially for long haul transmission. Nevertheless, this error may be canceled out to some extent *relying* on the estimate  $\widehat{D}$  by T-BC (6). The OTN control plane contains global route information, which may play an important role in the asymmetry calibration process [10]. The network management system (NMS) is responsible for configuring the network including the wavelength ( $\lambda$ ) assignment, collecting the mean fiber link delay ( $\widehat{D}$ ) by the T-BC, and processing the fiber link delay asymmetry ( $A(\lambda)$ ) in (8) to determine the asymmetry compensation in the timing chain. The sum of  $A(\lambda)$  in the timing chain can be written as

$$A_T(\lambda_f, \lambda_r) = A_1(\lambda_{f1}, \lambda_{r1}) + A_2(\lambda_{f2}, \lambda_{r2}) + \dots + A_N(\lambda_{fN}, \lambda_{rN}), \quad (15)$$

where  $A_i(\lambda_{fi}, \lambda_{ri}) = 0$  for  $\lambda_{fi} = \lambda_{ri}$ . An illustration of asymmetry compensation support from OTN control plane is shown in Figure 8.

The integrity of transferring accurate time/phase synchronization over OTN and PTN with Sync-E networks is shown in Figure 9. Figure 9 is based on the full timing support (e.g., T-BC) from the network architecture as described in ITU-T G.8275.1, with the addition of frequency support (e.g., syntonized T-BC) being considered to improve time/phase recovery accuracy [16, 17]. The timing chain normally would be 11 hops (e.g., 10 T-BCs) and can extend to 15 hops (e.g., 14 T-BCs); this requires tight time error components control [18]. T-BC corrects the time/phase in the various network nodes and also provides a set of performance metrics including mean path delay and current offset from master [14]. As the PRTC cooperate with PRC (shown in Figure 9), the coherence between the frequency and time/phase planes can be realized, and this allows extending the time/phase holdover period during GNSS failures. Furthermore, a unified IEEE1588v2 management approach offers a compelling set of operational advantages including the ability to perform end-to-end performance analysis and troubleshooting.

## 5. Conclusion

The In-band fiber link delay asymmetry due to the use of different wavelengths in the two directions should be taken into account, especially for long haul transmission. This introduces significant time error (i.e., phase offset) within 0.3397 ns/km in C-band or 0.3943 ns/km in L-band depending on the wavelength spacing.

With the proposed scheme in this paper, the fiber link delay asymmetry can be compensated relying on the estimated mean fiber link delay by the T-BC mode and the NMS to compute the delay asymmetry in the timing chain. To deploy IEEE1588v2, bidirectional protection switch can minimize link length asymmetry in contrast to unidirectional protection switch.

It is an essential prerequisite to shorten the number of a T-BC chain, which can limit the impact of asymmetries. Furthermore, the integrity of transferring accurate time/phase synchronization over OTN and PTN with Sync-E networks can simplify network architecture, reduce OPEX, and make the network easy to maintain.

## Conflict of Interests

The authors declare that there is no conflict of interests regarding the publication of this paper.

## Acknowledgment

This work is supported in part by the Bureau of Standards, Metrology and Inspection, Ministry of Economic Affairs, Taiwan (Grant no. BSMI 103-1403-05-05-01).

## References

- [1] A. Bari, J. Jiang, W. Saad, and A. Jaekel, "Challenges in the smart grid applications: an overview," *International Journal of Distributed Sensor Networks*, vol. 2014, Article ID 974682, 11 pages, 2014.
- [2] D. Schneider, "The microsecond market," *IEEE Spectrum*, vol. 49, no. 6, pp. 66–81, 2012.
- [3] P. Kartaschoff, "Synchronization in digital communications networks," *Proceedings of the IEEE*, vol. 79, no. 7, pp. 1019–1028, 1991.
- [4] A. Magee, "Synchronization in next-generation mobile backhaul networks," *IEEE Communications Magazine*, vol. 48, no. 10, pp. 110–116, 2010.
- [5] J.-L. Ferrant, M. Gilson, S. Jobert et al., *Synchronous Ethernet and IEEE 1588 in Telecoms: Next Generation Synchronization Networks*, Wiley-ISTE, 2013.
- [6] ITU-T Recommendation G.8275, *Architecture and Requirements for Packet-Based Time and Phase Delivery*, 2013.
- [7] ITU-T Recommendation G.709/Y.1331, *Interfaces for the Optical Transport Network (OTN)*, December 2009.
- [8] K. Hann, S. Jobert, and S. Rodrigues, "Synchronous ethernet to transport frequency and phase/time," *IEEE Communications Magazine*, vol. 50, no. 8, pp. 152–160, 2012.
- [9] J.-L. Ferrant, M. Gilson, S. Jobert et al., "Development of the first IEEE 1588 telecom profile to address mobile backhaul needs," *IEEE Communications Magazine*, vol. 48, no. 10, pp. 118–126, 2010.
- [10] S. Ruffini, "Time sync distribution via PTP challenges, asymmetries, solutions," in *Proceedings of the International Telecom Sync Forum (ITSF '11)*, pp. 3–37, 2011.
- [11] M. Ouellette, K. Ji, S. Liu, and H. Li, "Using IEEE 1588 and boundary clocks for clock synchronization in telecom networks," *IEEE Communications Magazine*, vol. 49, no. 2, pp. 164–171, 2011.

- [12] M. Ouellette, G. Garner, and S. Jobert, "Simulations of a chain of telecom boundary clocks combined with synchronous ethernet for phase/time transfer," in *Proceedings of the International IEEE Symposium on Precision Clock Synchronization for Measurement, Control, and Communication (ISPCS '11)*, pp. 105–113, Munich, Germany, September 2011.
- [13] K. Cochrane, J. E. Bailey, P. Lake, and A. Carlson, "Wavelength-dependent measurements of optical-fiber transit time, material dispersion, and attenuation," *Applied Optics*, vol. 40, no. 1, pp. 150–156, 2001.
- [14] "IEEE standard for a precision clock synchronization protocol for networked measurement and control systems," IEEE Std 1588-2008, Revision of IEEE Std 1588-2002, July 2008.
- [15] ITU-T Recommendation G.984.3, Amendment 2: Time-of-day distribution and maintenance and clarifications, 2008.
- [16] ITU-T Recommendation G.8251, "The Control of Jitter and Wander within the Optical Transport Network (OTN)," November 2010.
- [17] J.-L. Ferrant, G. M. Garner, M. Mayer, J. Rahn, S. Rodrigues, and S. Ruffini, "OTN timing aspects," *IEEE Communications Magazine*, vol. 48, no. 9, pp. 62–69, 2010.
- [18] ITU-T, Network Limits for Time Synchronization in Packets Networks, ITU-T Recommendation G.8271.1, 2013.





**Hindawi**

Submit your manuscripts at  
<http://www.hindawi.com>

